X-ray lithography beamlines in the IBM Advanced Lithography Facility

by J. P. Silverman R. P. Rippstein J. M. Oberschmidt

In 1991 a storage ring designed as a source of X-rays for X-ray lithography was delivered, installed, and commissioned in the IBM Advanced Lithography Facility (ALF) in East Fishkill, New York. Beamlines of two different designs have been constructed and installed on the ring to deliver the X-rays to the exposure stations. One design is intended for use with a stepper for the fabrication of integrated circuits. The second design is for a general-purpose research and development beamline which is used for unaligned exposures as well as for characterization of beamline components. The design and performance of both are described. Special attention is given to a paraboloid mirror optical system which is used to collimate the radiation from the storage ring. Both the theoretical and the measured performance of the mirror are presented and shown to be in excellent agreement. An exposure nonuniformity of less

than $\pm 3\%$, including contributions from both the mirror and the beryllium exit window, has been achieved.

Introduction

• Functions of a beamline

In synchrotron-based X-ray lithography, the X-rays are generated by the acceleration of electrons as they travel along a curved path through a dipole magnet in a storage ring [1]. The properties of the radiation [2] and the technical requirements on the operation of the ring impose a number of constraints on the extraction and use of the X-rays.

For example, an ultrahigh-vacuum (UHV) environment is required in the ring in order to maintain the beam with a long lifetime; otherwise, the electrons in the beam are quickly lost by scattering from gas atoms along their path. The wafer to be exposed, however, is inherently incompatible with a UHV environment. Exposure of the

**Copyright 1993 by International Business Machines Corporation. Copying in printed form for private use is permitted without payment of royalty provided that (1) each reproduction is done without alteration and (2) the Journal reference and IBM copyright notice are included on the first page. The title and abstract, but no other portions, of this paper may be copied or distributed royalty free without further permission by computer-based and other information-service systems. Permission to republish any other portion of this paper must be obtained from the Editor.

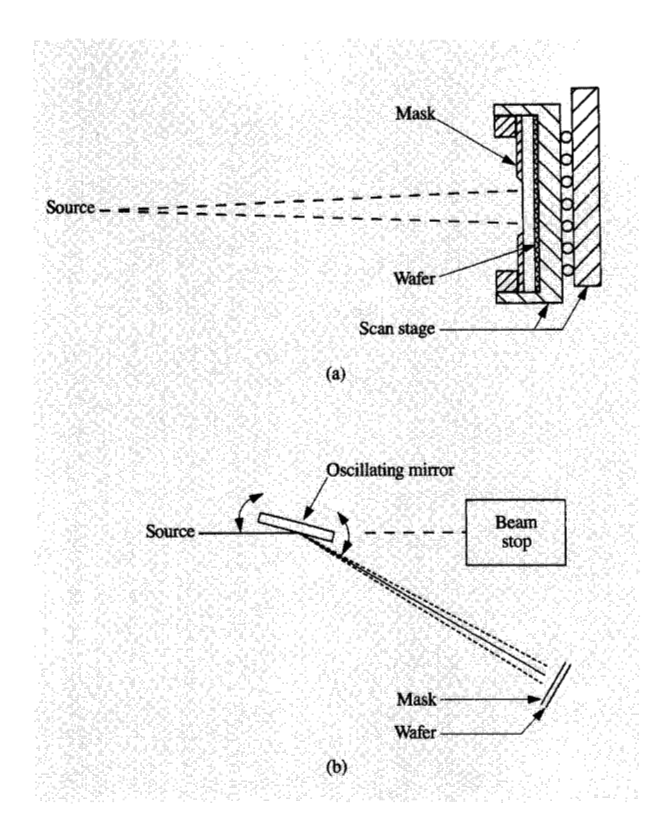


Figure 1

Methods to achieve vertical exposure uniformity: (a) Scanning of mask and wafer together through stationary beam. (b) Reflected radiation scanned across stationary mask and wafer by oscillating mirror.

photoresist coating on the wafer releases molecular fragments. Furthermore, the stepper which holds and aligns the mask to the wafer adds additional constraints on the wafer's environment. For example, some kind of cooling gas (e.g., air or helium) is required between the mask and wafer in order to thermally sink the mask to the wafer. Without this gas to provide heat transport, mask heating may cause unacceptable distortion. Another requirement is that the wafer must be held flat, which is generally accomplished by the use of a vacuum chuck (which in turn requires near-atmospheric pressure acting against the vacuum). The alternative is to use an electrostatic chuck, which can work in vacuum [3] but which makes wafer loading and unloading significantly more difficult. As a result, essentially all steppers now in operation or design work at atmospheric pressure.

The beamline is the interface between the ring and the exposure tool (e.g., the stepper). It delivers the X-rays from the ring through a vacuum barrier so that they can be used effectively for exposing resist. Thin beryllium foils

are most commonly used as exit windows because of their combination of high strength and low X-ray absorption. Furthermore, beryllium is UHV compatible as well as relatively immune to radiation damage. Any exit window, however, also acts as a filter and therefore alters the spectrum of transmitted radiation.

In addition to the vacuum function, however, a beamline can also include an optical system to optimize the flux delivered to the wafer. For example, collimating optical elements can be used to increase the amount of flux at the wafer and thus reduce exposure time. Also, depending on the stepper design, the optics may be required to provide uniform illumination of the exposure field. A high degree of uniformity is desirable in order to increase the latitude of the resist process, since the linewidth printed in resist of a given feature on the mask varies with dose. A nonuniformity of less than 3% is desirable today, and better than 1% may be required for future sub-0.25- μ m lithography.

The radiation emitted from the storage ring appears as a horizontally uniform stripe due to the symmetry of the circulating electron beam. Vertically, however, the intensity profile is Gaussian-like, with the width of the profile being a function of the wavelength of the radiation. For X-ray lithography, the useful wavelength is ~ 10 Å, where the vertical width of the beam is $\lesssim 1$ mrad. Thus, even 10 meters from the source, the height of the stripe is only ~ 10 mm, with a distinct Gaussian-like vertical intensity distribution. Exposure field sizes, however, are typically 25 mm or more in height, requiring some technique for providing uniform illumination over this area.

One technique now in use is to scan the mask and wafer together vertically through the beam [4], as illustrated in Figure 1(a). While this method gives excellent uniformity, the overhead associated with the scanning can significantly reduce the throughput of the stepper. Stability of the alignment during the scan is also a concern. The alternative is to use an oscillating mirror in the beamline, as shown in Figure 1(b). As the mirror changes its angle, the reflected beam is swept up and down over the wafer, with the ability to give good uniformity over a large area. The mirror must be used at grazing incidence in order to provide reasonable reflectivity. For a gold-coated mirror, reflectivities on the order of 70% can be expected for the wavelength range of interest for angles of incidence ≤25 mrad.

The use of a mirror also provides an additional advantage in safety. Although 10-Å X-rays do not penetrate through any significant amount of material (e.g., a piece of sheet metal can stop them effectively), there is a potential hazard due to Bremsstrahlung radiation generated when electrons in the storage ring undergo collisions with gas atoms or the wall of the vacuum chamber of the ring. In these cases, photons with energies up to that of the

electron beam (~700 MeV) can result. Such photons can be deeply penetrating; 10–20 cm of lead are needed to absorb their energy. Fortunately, these high-energy photons are highly collimated and are emitted only within a very narrow angular range around the plane of the circulating beam. Thus, a mirror can deflect the useful X-ray beam out of that plane, allowing installation of a beam stop to shield the Bremsstrahlung, as shown in Figure 1(b).

• Historical perspective

The first IBM beamline dedicated to X-ray lithography was installed in 1982 on Port U6 of the VUV storage ring at the National Synchrotron Light Source (NSLS) at Brookhaven National Laboratory [5, 6] and is still in use today. Originally intended to work with a stepper built at the IBM Thomas J. Watson Research Center [3], it was designed for exposures in a low-pressure (~20 torr) helium environment. A thin ($\sim 20 \mu m$) beryllium foil 54 mm in diameter is used as an exit window to separate the UHV portion of the beamline from the exposure chamber and stepper. Such a large, thin window is not capable of supporting an atmosphere of differential pressure, requiring exposures to be done in vacuum or at low pressure. Protecting the window from being subjected to atmospheric pressure also requires additional complexity of the vacuum system design and interlocks.

An oscillating mirror located 2.7 m from the source point in the ring is used to provide uniform illumination. The mirror has a cylindrical figure in order to collimate the radiation and increase the flux at the wafer plane. The focal length of a cylindrical mirror is given by the equation

$$f=\frac{r}{2\sin\theta},$$

where r is the radius of the cylinder and θ is the angle of incidence. Thus, for r=13.4 cm and f=2.7 m, good collimation of radiation from a point source is achieved at a grazing angle of incidence of 25 mrad. As the mirror angle changes during scanning, the reflected beam is slightly divergent (at shallower angles) or convergent (at steeper angles). The scan speed must therefore be a function of position in order to correct for the effective intensity changes that result. This system has achieved $\pm 7\%$ nonuniformity over a 25 \times 25-mm² field at a scan rate of 24 Hz.

Operating in a research mode, this beamline was used with the home-built stepper to fabricate the first working circuits that used synchrotron radiation to pattern all the levels of the circuits [3]. It has also been used extensively for resist characterization and studies of radiation damage to both masks and fabricated devices.

The IBM X-ray lithography effort continued in 1989 with the delivery of a commercially available stepper [7] which scans the mask and wafer vertically through a stationary beam. To accommodate this stepper, a second beamline was designed, constructed, and installed at Port U2 of the NSLS [8]. It features a toroidal mirror (which collimates the radiation in both the vertical and horizontal planes) and a beryllium exit window which is curved to match the curved stripe of radiation that is reflected from the toroidal mirror. Because the 20- μ m-thick window is only \sim 15 mm high, it can withstand atmospheric pressure, allowing it to be used with a stepper that operates in an atmospheric environment.

A major objective in building this beamline was to develop a more production-worthy design. In particular, the control system was designed to be more sophisticated and extendible than those found on other beamlines. Much of what was learned in the construction and operation of this beamline formed the basis for the design of the beamlines in the ALF today. A second major objective was the use of the beamline for fabrication of test circuits, including 1-Mb DRAMs [9].

Meanwhile, X-ray lithography beamlines have been developed at other synchrotron facilities around the world. At BESSY in Berlin, for example, a planar scanning mirror has been used [10], while NEC has used a cylindrical scanning mirror on a beamline at their Photon Factory in Tsukuba, Japan [11]. Another design [12] calls for a fixed toroidal mirror to collimate horizontally while expanding the beam vertically, though the authors suggest that the mirror could be scanned as well. Multimirror optical systems have also been proposed and in some cases tested. The University of Wisconsin originally proposed a three-mirror system [13] in which the first and last mirrors are planar while the middle mirror focuses the beam. That design has been supplanted by another three-mirror system [14] in which the first two mirrors are toroids and the third mirror is an optional scanning planar mirror. A beamline with this design is now in operation [15] at the Aladdin storage ring in Stoughton, Wisconsin. NTT has constructed a beamline at their own storage ring facility in Atsugi, Japan, that uses two toroids, the second of which scans [16, 17].

The ALF [18] was specifically designed to house the Helios storage ring [19] and to be the focal point for IBM X-ray lithography development. The beamlines now in operation in the ALF were designed for two separate purposes. This paper discusses the designs and performance of these beamlines, with emphasis on a paraboloid mirror optical system used to collimate the beam.

Design goals for beamlines in the ALF

Of the two types of beamlines in the ALF, the most common, called the ALF beamline, was designed [20] for use with an improved version of the stepper that has been

397

used at Beamline U2 at the NSLS. This stepper also scans the mask and wafer together through a stationary beam. The design objectives are optimized throughput with excellent horizontal uniformity of illumination. Furthermore, the ALF beamline is intended to be production-worthy, meaning that it can be readily replicated as needed. Indeed, three beamlines of this design are now installed in the ALF. One stepper is now operational, with a second currently undergoing commissioning.

The second beamline type, called the RD beamline, is a general-purpose beamline that can be used for unaligned exposures as well as for characterization of beamline components such as mirrors and exit windows. It is both more flexible and more complex than the ALF beamline design, and changes can be made as necessary to test new ideas without impact on the exposure capacity provided by the ALF beamlines. Since testing mirrors is one of its primary purposes, it has been designed to allow exposures in high vacuum, thus allowing exposures without an exit window. This capability avoids the confusion that can be caused by convolving effects of the window with those of the mirror.

Each beamline must meet the UHV requirements imposed by the operating requirements of the storage ring. The vacuum level in the beamline depends on whether or not it is open to the beam, since the X-rays in the beam cause significant desorption of gas where they strike the surfaces in the vacuum chamber. A pressure limit near the ring of 7×10^{-10} torr without beam has been established to initiate beamline operations. (Alternatively, a total pressure as high as 2×10^{-9} torr is permitted as long as the pressure due to species with atomic mass greater than 27 is less than 5×10^{-10} torr.) Additionally, the beamline is constrained by the physical layout of the ALF, most notably by the thick wall of the vault in which the storage ring is located. While lead is effective at absorbing Bremsstrahlung, the absorption process can produce neutrons which are emitted more isotropically but only weakly absorbed. To stop the neutrons, a concrete shielding wall ~2 m thick is located ~4.5 m from the beamline port on the ring (\sim 5.5 m from the source point). The beamline must pass through a hole in the shielding wall, which is then backfilled with radiation-absorbing material, making routine access to this portion of the beamline extremely difficult.

The controls for the beamlines [20] were designed for compatibility with the other control systems in the ALF (e.g., the safety system and the separate front-end control system). Both hardware and software were supplied to IBM specifications by vendors, with production-worthiness again as a goal. There are four basic levels of controls. At the most basic level are vendor-supplied controllers of individual components, such as vacuum pumps and

gauges. The next level of control is a programmable logic controller (PLC), which is used to implement the beamline interlocks. The PLC also provides certain timing functions as well as some diagnostic information. The user interface to the PLC is through FIX DMACS™, ¹ a software package that provides a graphical representation of the beamline and allows the operator to control individual components such as valves, pumps, and gauges. Finally, programmed sequences of operations are implemented in POMS®, ² a process-management software package which also has a graphical user interface. Both FIX DMACS and POMS run concurrently in an IBM PS/2® computer using the OS/2® operating system. Communications among the PS/2, the PLC, and other control systems is done over a local area network (LAN).

Front ends

The front end is the portion of the beamline that provides the vacuum and safety interface to the storage ring. All beamlines currently installed have nearly identical front ends, though it is conceivable that future special-purpose beamlines might have specialized front ends as well. Listed in order going downstream from the synchrotron there are five major components: a UHV gate valve, a photon mask, a second UHV gate valve, a "fast" valve, and a safety shutter. The first gate valve is operated in a manual mode and is used to seal off the ring from the beamline when maintenance on the front end is required upstream from the second gate valve. Otherwise it is always left open, since the ring is not operable with it closed; the intense radiation striking the valve gate could damage it and cause it to leak. The photon mask is used to absorb the radiation and to protect valves farther downstream when they are closed. It consists of a water-cooled copper block which is mounted on a piston to allow it to be lowered out of the beam when flux is desired down the beamline. As an added feature, the copper block has been polished and mounted at 45° to the beam so as to reflect the visible portion of the spectrum up through a viewport for diagnostic purposes.

The second gate valve operates under automatic control and is the valve normally used to seal off the beamline as required. However, this gate valve operates relatively slowly, taking ~3 s to close. In case of a vacuum accident in a beamline, its response would be too slow to protect the storage ring from vacuum contamination. Since the ring has superconducting magnets with a cold bore [19], a serious vacuum accident would not only cause a quench of the superconducting dipole magnets but could also contaminate the ring vacuum to the point where a bakeout would be required. The resulting downtime would be

¹ FIX DMACS (Fully Integrated Control System, Distributed Manufacturing, Automation, and Control Software) is a product of Intellution, Inc., Norwood, MA. ² POMS is an IBM Licensed Product marketed and produced by IBM. It is developed by Incode, Inc., Reston, VA.

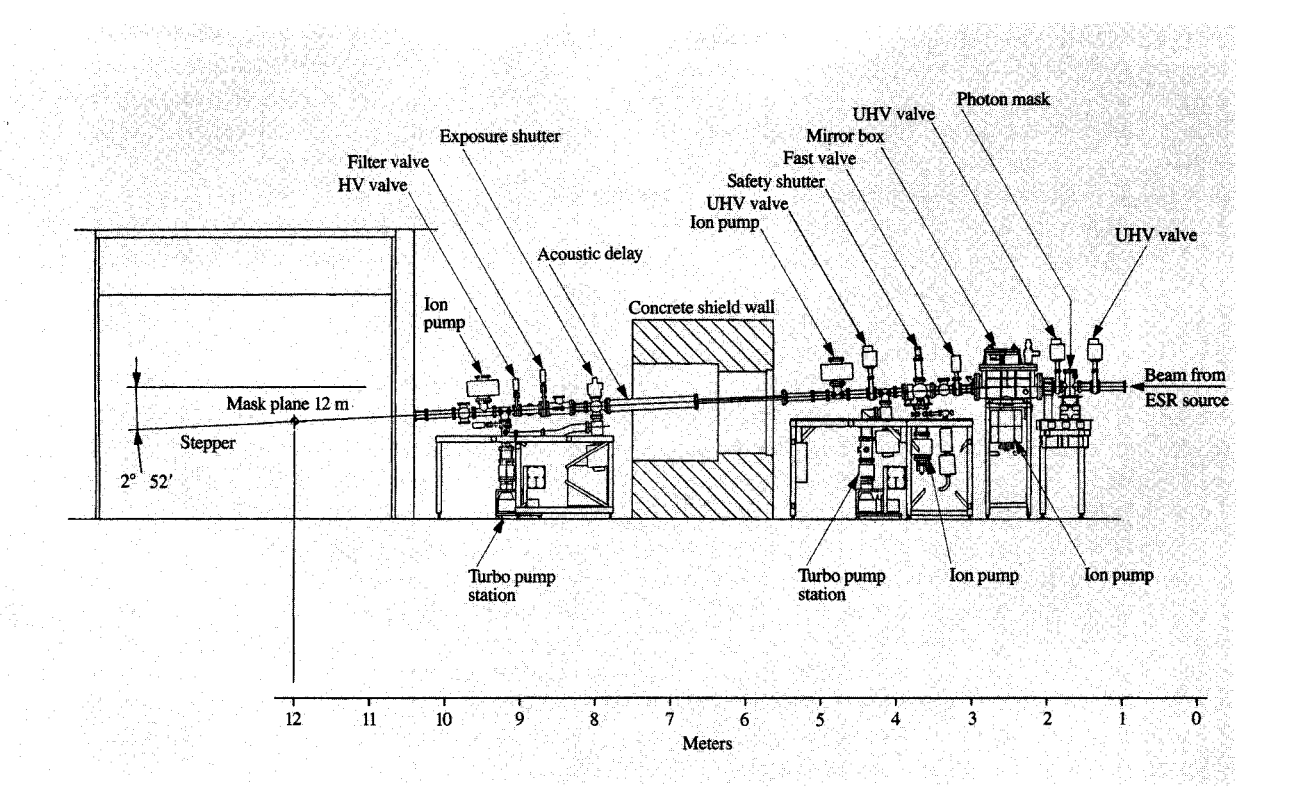


Figure 2

Layout of the ALF-type beamline.

unacceptable in a heavily used facility. Therefore, a fast-acting valve has been installed as well. When triggered by a pressure rise on a dedicated sensor located near the beryllium window, this valve closes in ~10 ms. While it does not make a UHV seal, it does severely limit the conductance and therefore the damage caused during the time the gate valve takes to seal.

Finally, the front end includes a safety shutter for additional radiation protection. Consisting of a block of tungsten mounted on a piston, it is inserted into the beamline while electrons are injected into the ring, which is when the radiation levels are highest. It thus blocks the hole in the shield wall created by the beamline itself and stops any Bremsstrahlung remaining at that point. The remaining solid angle through which neutrons could pass down the beamline is consequently reduced to an acceptably low value.

In addition, pumping and vent valves are included in the front end, as are pumps, pressure gauges, and some diagnostic equipment. Another beamline isolation gate valve located downstream from the front end is also controlled by the front-end control system.

The ALF beamline

The layout of the ALF beamline is shown in Figure 2. Because of space constraints and the need to optimize the performance of optical systems, the mirror box (in which the mirror is mounted) is located 2.6 m from the source in the middle of the front end between the second UHV valve and the fast valve. The mirror is normally fixed (i.e., it does not scan) but can be adjusted or scanned with stepping motors. A 25-µm-thick beryllium exit window that can withstand atmospheric pressure is used for compatibility with the stepper, in which the exposure plane is located ~12 m from the source. In addition, a second beryllium foil 10 μ m thick has been installed ~3 m upstream from the exit window. This upstream filter is mounted on a modified gate valve so that it can be inserted in or removed from the beam as desired. It is routinely left in the beam both to absorb the low-energy part of the spectrum (which would not penetrate the exit window but which would cause heating) and to provide an additional barrier to any helium (which is used to flush the area downstream from the exit window) that might leak in through the exit window. Because of the potential for a

399

vacuum accident caused by a rupture of a window, an acoustic delay line (ADL) has been installed upstream from the exit window. The interior of the ADL is a series of angled baffles that slow the shock wave that would result from such an accident, providing enough delay to allow the fast valve to close before the ring vacuum is seriously contaminated.

The exit window is also curved to match the shape of the beam as reflected from a paraboloid mirror, as is discussed in more detail below. At present, however, a planar mirror has been installed in the mirror box, pending delivery of the paraboloid. Since the full height of the beam is >10 mm, the mismatch between the shape of the window and the shape of the stripe of radiation causes some amount of radiation to be blocked at the bottom of the beam in the center of the field and at the top of the beam at the edges. The mirror has consequently been adjusted to optimize the flux uniformity over a 30-mm-wide field. Both flux and uniformity have been measured by exposing a radiachromic film [21] and measuring the resulting optical density in either a calibrated densitometer (for flux) or on a scanning densitometer (for uniformity). The resulting horizontal uniformity over this field has been found to be $\pm 1.4\%$, not including a high (>1/mm) spatial frequency contribution of about $\pm 2\%$ attributed to thickness variations due to the grain structure of the beryllium windows. The vertical uniformity, which depends on the constancy of the scan speed of the stepper as well as on the purity of the helium environment downstream from the exit window, was measured to be $\pm 0.5\%$. Note that if the helium is contaminated with air, both the uniformity and the total flux delivered can suffer. The total flux is characterized by the equation

$$s = \frac{IT}{kD},$$

where s is the scan speed of the stage (in mm/s), I is the stored current in the ring (in mA), T is the transmission of the mask (between 0 and 1.0), k is a calibration constant, and D is the requested dose (in mJ/cm²). Using the planar noncollimating mirror, k has a measured value of 0.42, which is equivalent to a mask-incident flux of 48 mW/cm (96 mW total) over a 2-cm-wide field at a typical stored current of 200 mA (the ring is routinely filled to ~250 mA and has a beam lifetime in excess of 10 hours [22]). With a typical mask transmission of ~0.42 (i.e., ~42%), a 25-mmhigh field requiring 100 mJ/cm² deposited in the resist would take a 12.5-s exposure at 200 mA, for an effective flux rate of 8 mW/cm² delivered to the resist (not including time for overscanning). This flux rate could be increased by the use of a collimating mirror (discussed in more detail below) or by removing the upstream filter from the beam.

Since the stepper controls the exposure, both by setting the scan speed and by use of another beam shutter, routine operation of the beamline involves only short daily start-up and shutdown procedures which open and close the appropriate valves. No POMS-level sequencing procedures have yet been implemented, though they are planned for the near future.

The RD beamline

The RD beamline has a number of features that distinguish it from the ALF beamline, as illustrated by the layout shown in Figure 3. As with the ALF beamline, the mirror box, which houses a fixed mirror, is located 2.6 m from the source in the middle of the front end. In contrast, however, there is no stepper, so a special vacuum chamber has been installed at the end of the beamline (~13 m from the source) for exposures. A linear stage mounted inside the chamber allows samples to be scanned vertically through the beam, much as is done by the stepper at the end of the ALF beamline. Exposures are done either in vacuum (pressures as low as 10^{-7} torr have been achieved) or in a low-pressure (~20 torr) helium environment; indeed, the present beryllium exit window (20 μ m thick with an aperture 68 mm in diameter) will not withstand a full atmosphere of differential pressure, ruling out atmospheric exposures. As with the ALF beamline, provision has been made to install an acoustic delay line (ADL) just upstream from the beryllium window. Modifications which would allow the installation of a window capable of withstanding atmospheric pressure are also under consideration.

Since one of the main purposes of this beamline is to characterize mirrors, the window itself is mounted on a modified gate valve (like the upstream filter on the ALF beamline) which allows it to be removed from the beam. This allows exposures without introducing nonuniformities due to the window, since the differential pumping in the beamline permits operation with exposure chamber pressures as high as 10⁻⁶ torr. The operation of the RD beamline is significantly more complex than that of the ALF beamline, since the exposure chamber must be pumped out each time a sample is loaded. To ease the burden on the operator and allow personnel with minimal training to conduct experiments, POMS-level software has been implemented to perform automatically the sequence of steps necessary for exposure, including adjusting the speed of the scanning stage to provide the proper dose. Multiple scans are used as necessary for large doses (e.g., for some radiation damage exposures) due to the allowed range of stage scan speeds.

In addition, two filters are mounted on modified gate valves upstream from the beryllium exit window, so that they can be individually inserted or removed from the beam as desired. The filters can be used to alter the spectrum of the beam as well as to absorb power and to provide improved differential pumping. At present, the

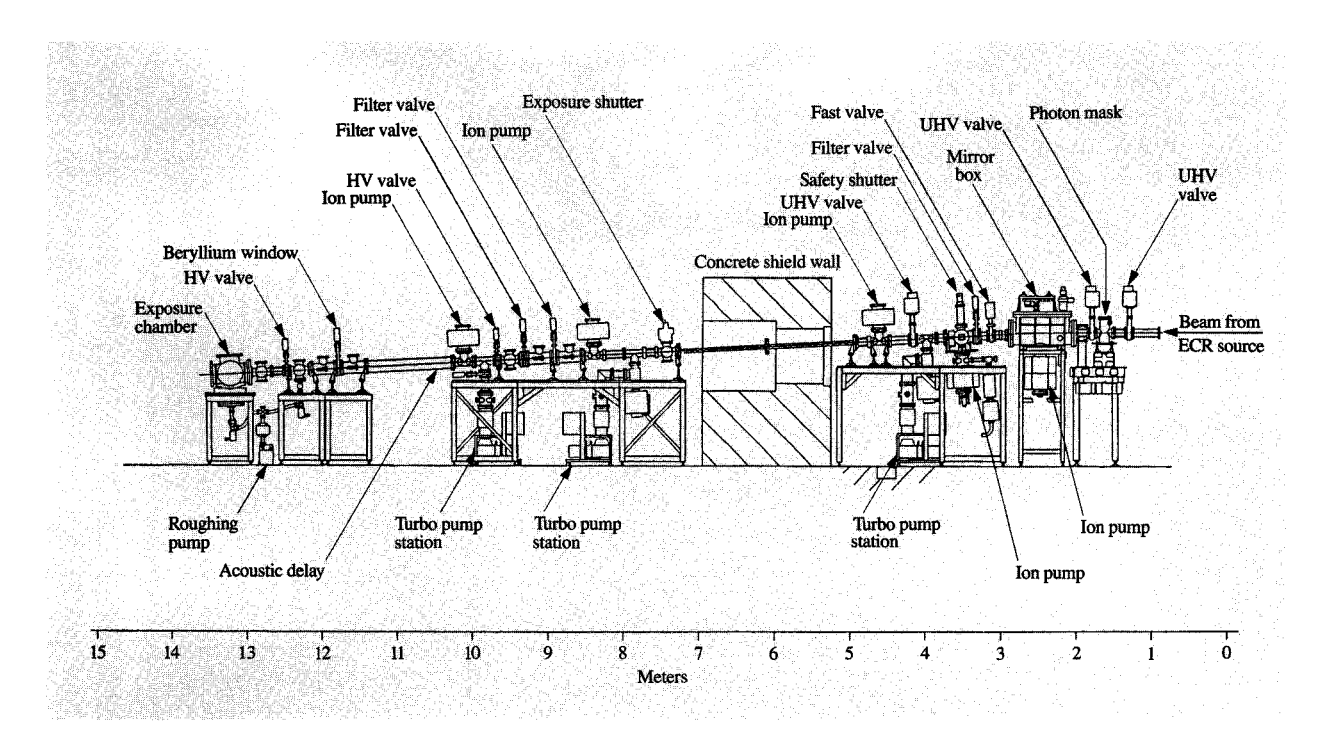


Figure 3

Layout of the RD-type beamline.

filters are both thin beryllium foils which are normally left out of the beam, being inserted only for special purposes.

The vacuum level in the beamline has been measured to be $\sim 1.5 \times 10^{-9}$ torr without beam, while it rises to levels of $\sim 1.8 \times 10^{-8}$ torr when opened to the beam at 250 mA of stored current. Some amount of "conditioning," i.e., exposing the beamline to beam at low current to limit the pressure rise due to photon-induced desorption, was initially required to keep the pressure levels from rising too high. However, adherence to proper vacuum techniques followed by a good bakeout has kept the conditioning time small; typically only a few hours of low-current operation are required following maintenance which breaks the vacuum.

Since there is no narrow exit window, excellent uniformity is expected and indeed obtained when a planar mirror is used. With a planar mirror installed in the mirror box and a previously installed 50- μ m-thick beryllium exit window, the uniformity measured over a 60-mm-wide field was found to be $\pm 3.1\%$ (including the contribution from the window itself), again attributed almost entirely to thickness variations in the beryllium. Measured with a different 20- μ m-thick window, the calibration constant k was found to be 0.26, corresponding to a mask-incident flux of 77 mW/cm at 200 mA over the 6-cm-wide field.

Advanced optics

While planar mirrors are simple, they have a distinct drawback in that they are inefficient at delivering flux to the wafer. The beam from the storage ring continues to spread out, wasting most of the flux coming out of the port. A figured mirror can collect and direct X-rays from a much larger acceptance angle. This collimation can result in as much as a factor of 5 or more increase in the delivered flux, depending on the design and the length of the beamline.

As mentioned above, various shapes can be used to collimate the radiation, either as single mirrors or in combinations. Both approaches have advantages and drawbacks. A single-figured mirror system, for example, has the disadvantage that the reflected stripe of radiation is curved, which requires that the scanning mechanism (either the mirror or the scanning stage) overscan in order to have the entire width of the field scanned by the entire beam. The effective duty cycle and corresponding throughput are reduced by the amount of overscan, as shown in **Figure 4**. To illuminate uniformly an area of height H, the total scan length must be

$$L_{s} = H + W + S,$$

where W is the width of the beam at the exposure plane

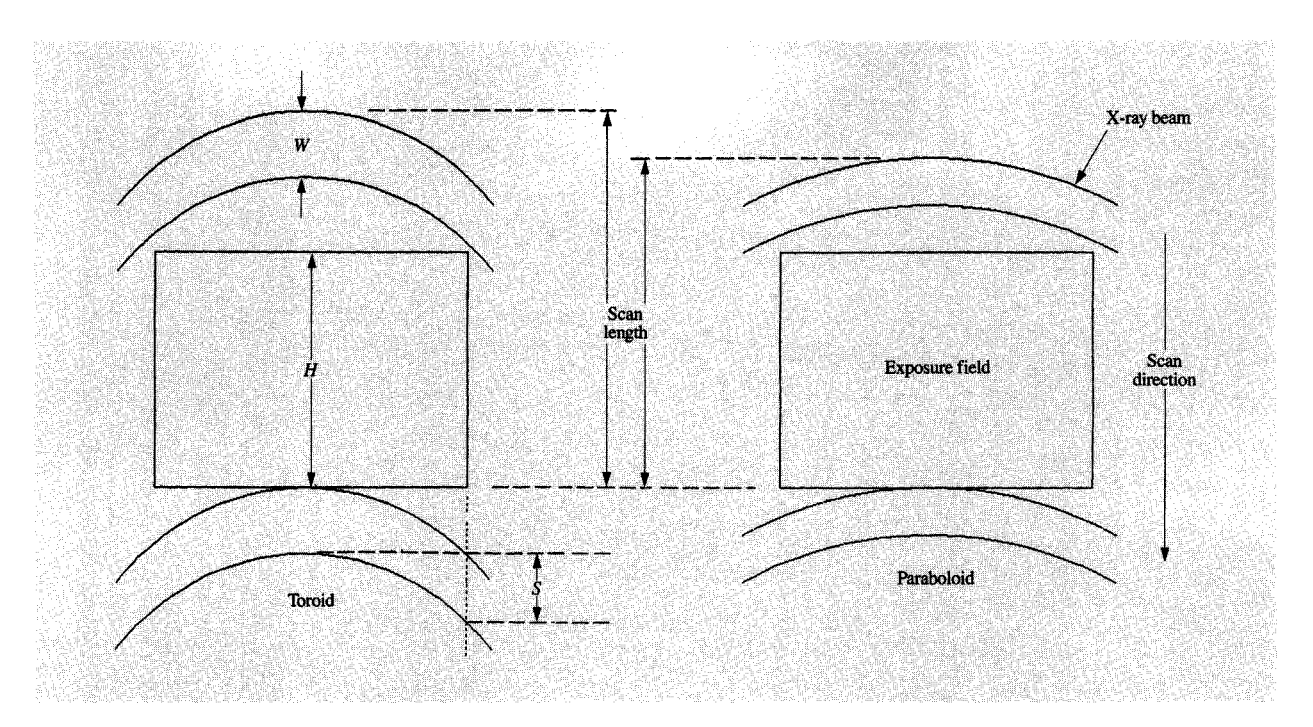


Figure 4

Effect of curvature of reflected beam profile on efficiency of scanning required to uniformly illuminate field. Scan efficiency is given by H/(H + W + S).

and S is the amount of "sag" of the reflected beam due to its curvature. An effective scan efficiency E can be defined as $E = H/L_{\rm s}$. Flatter and narrower beams are clearly advantageous. However, while a multimirror system can produce a flat stripe of radiation [15], the flux loss due to the finite reflectivity of the additional mirror also reduces throughput. Moreover, multimirror systems can introduce additional cost and complexity to the overall beamline design and implementation. For these reasons, a single-mirror system was chosen for the ALF beamlines.

There were two major constraints in the design of the optics. First, the nominal angle of incidence needs to be \lesssim 25 mrad to provide reasonable reflectivity. In addition, the physical layout of the ALF constrains the mirror to be located no closer than \sim 2 m from the source; other beamline space considerations strongly suggested that the source-to-mirror distance be no more than \sim 2.6 m. There were also a number of design goals:

- Collimation of flux for high throughput.
- Uniform illumination over a 60-mm-wide field.
- Minimal overscan due to curvature of reflected beam.
- Ability to use same mirror in either fixed-position or scanning mode (for a 25-mm-high field).

• Minimal distortion of field in either fixed or scanning mode.

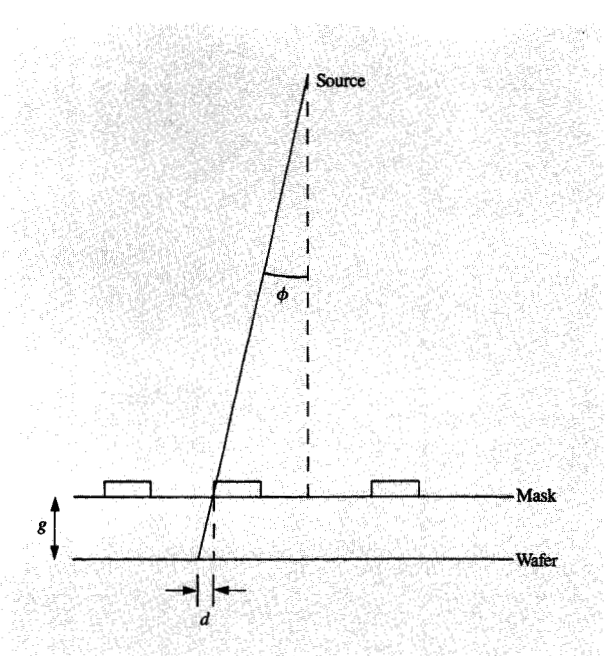
Distortion of the printed field on the wafer can arise if the rays reflected from the mirror are not truly collimated. If they converge or diverge, the printed pattern is displaced, as shown in **Figure 5**, by a distance

$$d = g \tan \phi$$
,

where g is the gap between the mask and wafer during exposure (typically $\sim 20-50~\mu m$) and ϕ is the "runout angle," i.e., the angle of the ray relative to the normal to the wafer plane. Depending on the gap and the amount of convergence or divergence, this distortion could be a large fraction of the overlay error budget at sub-0.25- μm dimensions.

Cylindrical, toroidal, and paraboloid mirrors were considered. For a toroidal mirror with focal length f operating at angle of incidence θ , the major radius R and minor radius r are given by

$$R = \frac{2f}{\sin \theta}$$



ioure 5

Runout (distortion of printed image) caused by radiation at an angle ϕ from the normal to the exposure plane.

and

$$r = 2f \sin \theta$$
.

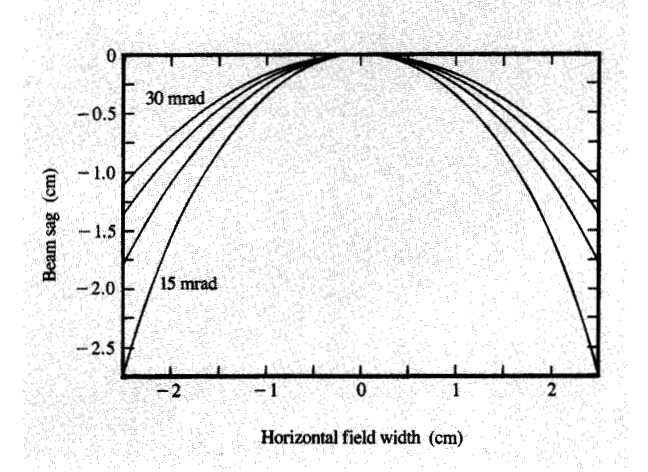
Note that a cylinder is simply a toroid with infinite major radius and focal length, so it is not considered separately. The equation for a paraboloid is

$$r^2 = 2pz + p^2,$$

where z is measured along the axis of the paraboloid and p is given by

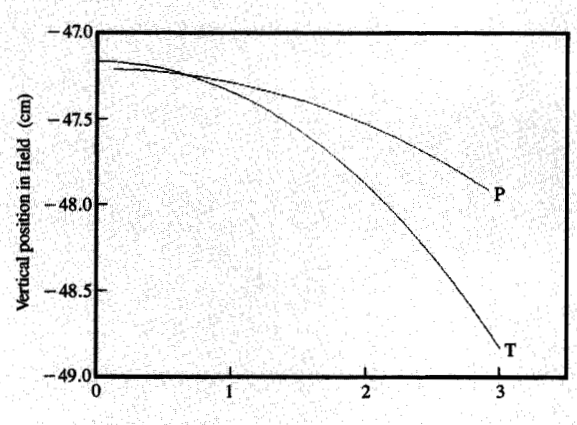
$$p = \frac{2f\cos 2\theta \tan^2 \theta}{1 - \tan^2 \theta}.$$

The predicted source size of the electron beam $(\sigma_x = 0.63 \text{ mm} \text{ and } \sigma_y = 0.53 \text{ mm})$ and angular emittance $(\sigma'_x = 3.2 \text{ mrad and } \sigma'_y = 0.4 \text{ mrad})$ as well as the worst-case size and emittance $(\sigma_x = 0.59 \text{ mm}, \sigma_y = 1.55 \text{ mm}, \sigma'_x = 2.9 \text{ mrad}, \text{ and } \sigma'_y = 0.4 \text{ mrad})$ [23] were input parameters for the modeling of the performance, which used both an internally written ray-tracing program and the SHADOW program [24] written at the University of Wisconsin. Since the amount of sag decreases as the grazing angle increases (**Figure 6**), the grazing angle was set to 25 mrad, near the maximum allowed before the reflectivity starts to decrease noticeably. As a result of the



Figure

Effect of angle of incidence (for 15, 20, 25, and 30 mrad) on amount of sag of reflected beam profile for a collimating cylindrical mirror.

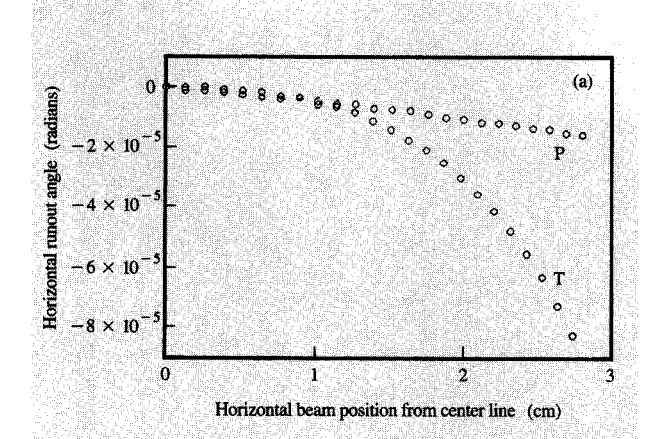


Horizontal beam position from center line (cm)

Figure 7

Comparison of modeled sag of paraboloid (P) and toroidal (T) mirrors. Beam is symmetric about center line in horizontal direction.

modeling, a source-to-mirror distance of 2.6 m was chosen. A comparison of the sag for the optimized toroid and paraboloid is shown in **Figure 7**. As can be seen, the paraboloid has significantly less curvature, especially for field widths greater than 3 cm. The horizontal and vertical



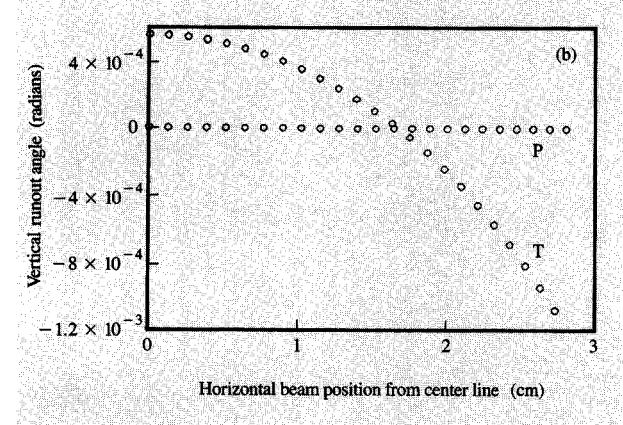


Figure 8

Comparison of (a) horizontal and (b) vertical modeled runout angles for paraboloid (P) and toroidal (T) mirrors.

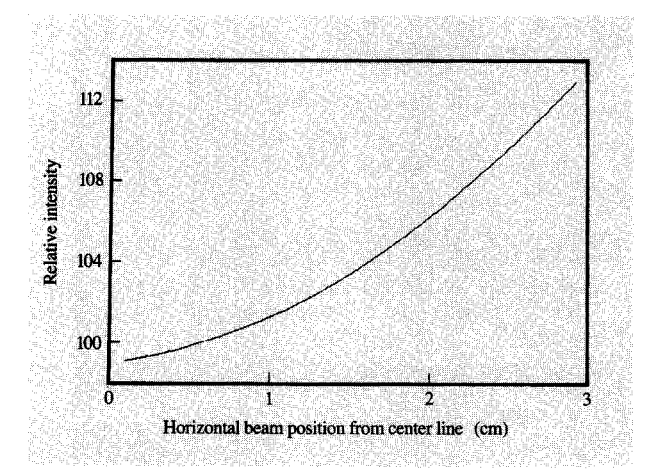


Figure 9

Modeled horizontal intensity of reflected beam as function of horizontal position for a paraboloid mirror.

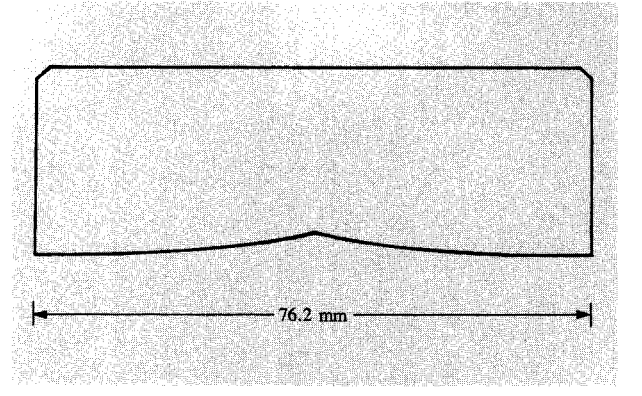


Figure 10

Shape of vignetting plate required to provide uniformity with paraboloid mirror, calculated from results shown in Figure 9. The beam passes below the plate, which blocks more of the beam at the edges than at the center.

Table 1 Mirror design parameters.

Mirror figureParaboloid of revolution,
p=3.2 mmSource-to-mirror distance2.6 mNominal grazing angle25 mradMirror active area70 mm wide \times 450 mm longDesign field size25 mm high \times 60 mm wideMirror coating10 nm evaporated Cr/60 nm
evaporated Au

runout angles for these same mirrors are shown in Figure 8; again, the paraboloid is clearly the preferred mirror, having much smaller and more constant runout angles. (The lack of perfect collimation by the toroid is due to the fact that the source-to-mirror distance is actually a function of lateral position when the mirror is used at grazing incidence.) Consequently, the paraboloid was chosen for use in the ALF beamlines. Its design parameters are shown in Table 1.

Although this design does minimize the sag and the runout angles, the horizontal uniformity as reflected from the mirror is relatively poor, with the intensity rising at the edges of the field as shown in **Figure 9**. However, the uniformity can be corrected by selectively vignetting the beam, i.e., inserting a shaped plate or aperture in front of the mirror to block part of the beam where the intensity is highest. Similar techniques have been used frequently in optical lithography to achieve good illumination uniformity. The shape of the vignetting plate (shown in **Figure 10**) has been modeled on the basis of the calculated nonuniformity shown in Figure 9. In principle, the correction can be essentially perfect for a stationary mirror. **Table 2**

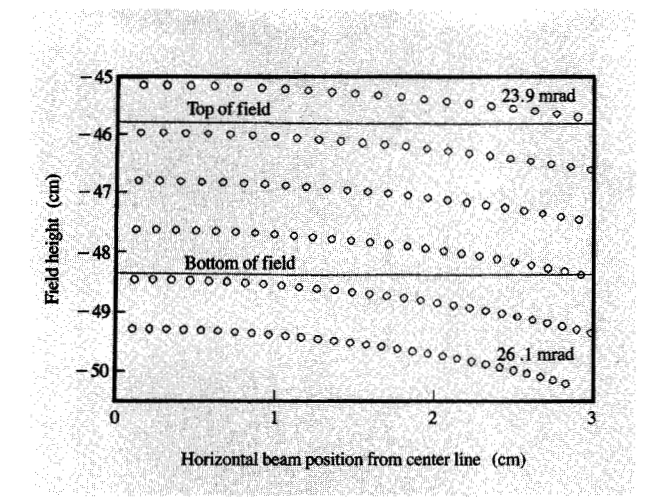


Figure 11

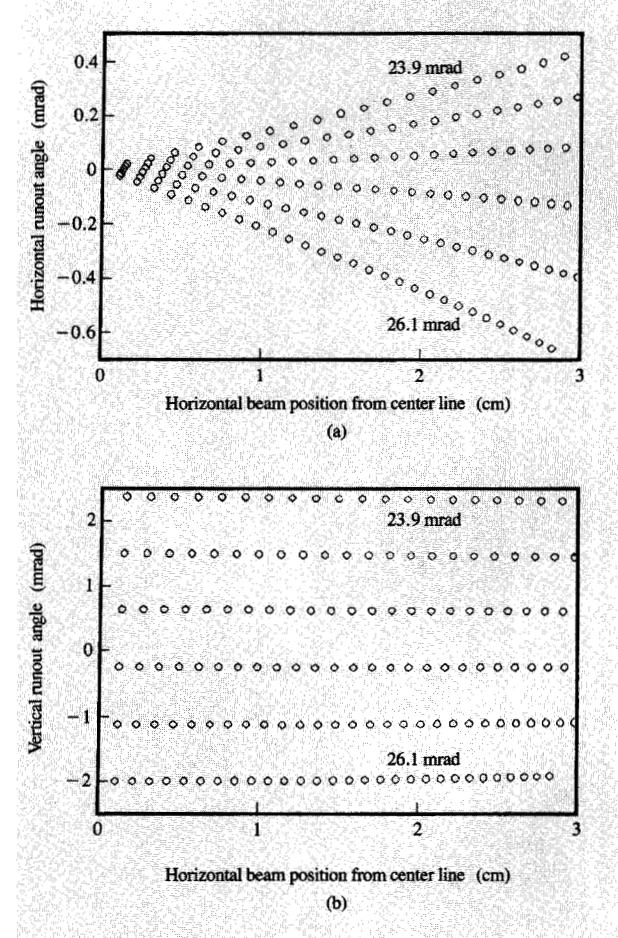
Modeled wafer plane beam profile as a function of vertical position resulting from scanning of paraboloid mirror.

Table 2 Modeled mirror performance (stationary).

Vertical beam size	less than 17 mm
Beam width	less than 10 mm ($\pm 3\sigma$)
Beam sag	7 mm at edges of 60-mm-wide field
Induced distortion (20-μm gap)	less than 1 nm
Blur (horizontal)	$0.73 \text{ mrad } (3\sigma)$
Blur (vertical)	$0.48 \text{ mrad } (3\sigma)$

summarizes the predicted performance of the mirror when stationary. Here "blur" represents the range of angles seen at a given point on the wafer (including contributions from the source size and emittance), and the induced distortion is calculated assuming a mask-to-wafer gap of $20~\mu m$.

The performance of the mirror in a scanning mode has also been modeled. The amount of sag has been found to vary slowly with angle over the angular range (about ± 1 mrad) required for a 25-mm field height, as illustrated in Figure 11. The uniformity and flux intensity also vary with mirror angle, but a nonuniform scan speed can be used to achieve better than $\pm 3\%$ illumination nonuniformity over a 25-mm-high field. The horizontal runout angle is a function of both mirror angle and x position, as illustrated in Figure 12(a), while the vertical runout angle is proportional to the deviation from the nominal angle of incidence (25 mrad) but independent of x position [Figure 12(b)]. In the worst case (at the corners of the field), the runout translates into a distortion of -30 nm. If, however, a nonisotropic magnification and trapezoid correction are made to the



Modeled (a) horizontal and (b) vertical runout angles for different scan angles of a paraboloid mirror.

Table 3 Modeled mirror performance (scanning).

Scan range to cover 25-mm field height	+1.1/-0.8 mrad	
Induced distortion	less than 31 nm at edges of	
(20-μm gap)	60-mm-wide field	
Corrected distortion	less than 12 nm with	
(20-μm gap)	nonisotropic magnification	
Blur (horizontal)	0.75 mrad	
Blur (vertical)	0.50 mrad	
Exposure uniformity	less than ±3% with vignetting aperture and scan velocity	
	correction	

mask, the distortion can be reduced to ~ 10 nm. The expected scanning performance of the mirror is summarized in **Table 3**.

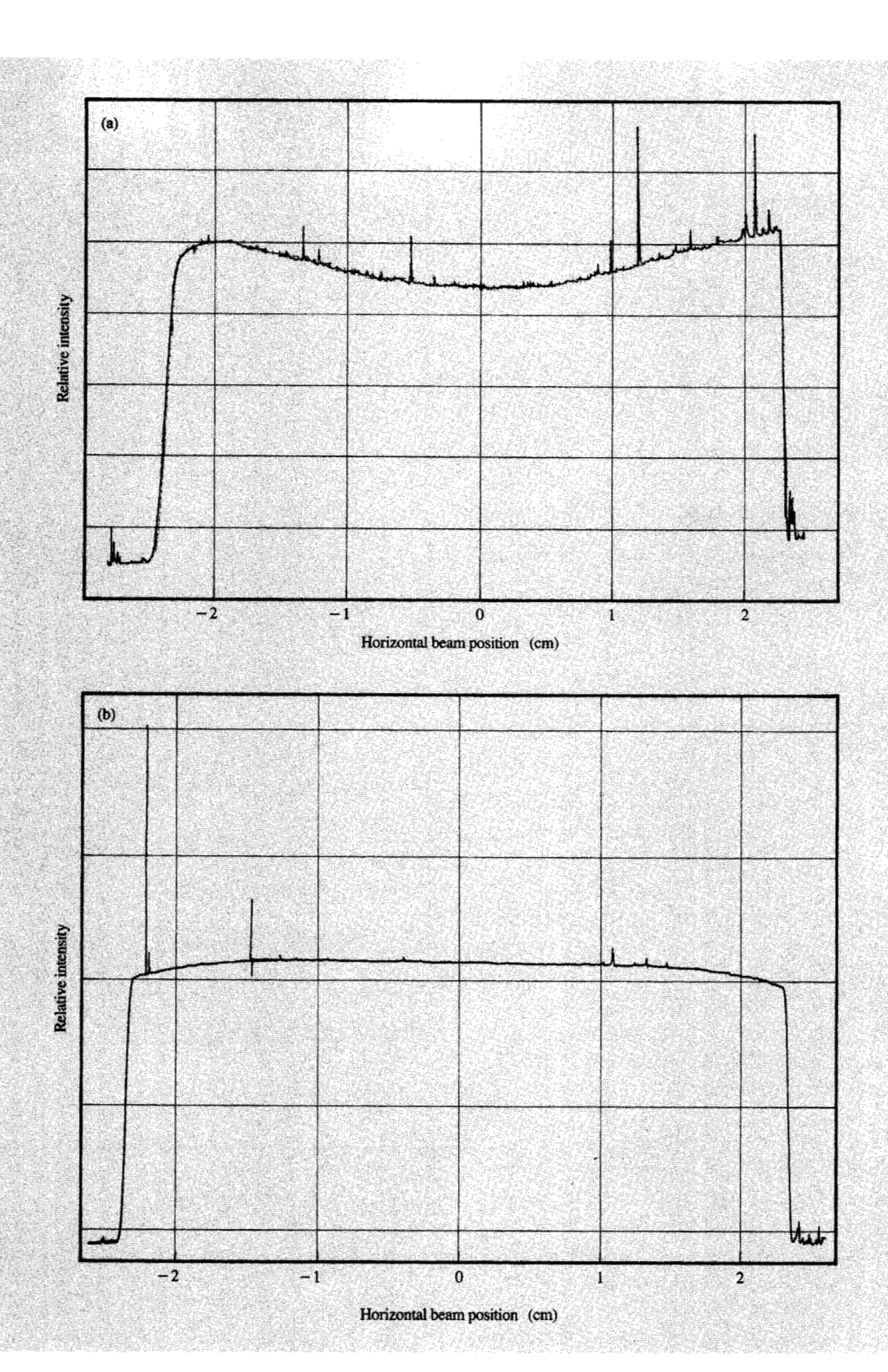


Figure 13

Measured horizontal uniformity of beam reflected from paraboloid mirror: (a) without vignetting, (b) with vignetting and with the beryllium exit window removed. The small-scale structure in (a) is attributed to variations in thickness of the beryllium window; note the absence of such structure in (b) with the window removed. The larger sharp spikes are due to dust on the film during measurement in the scanning densitometer.

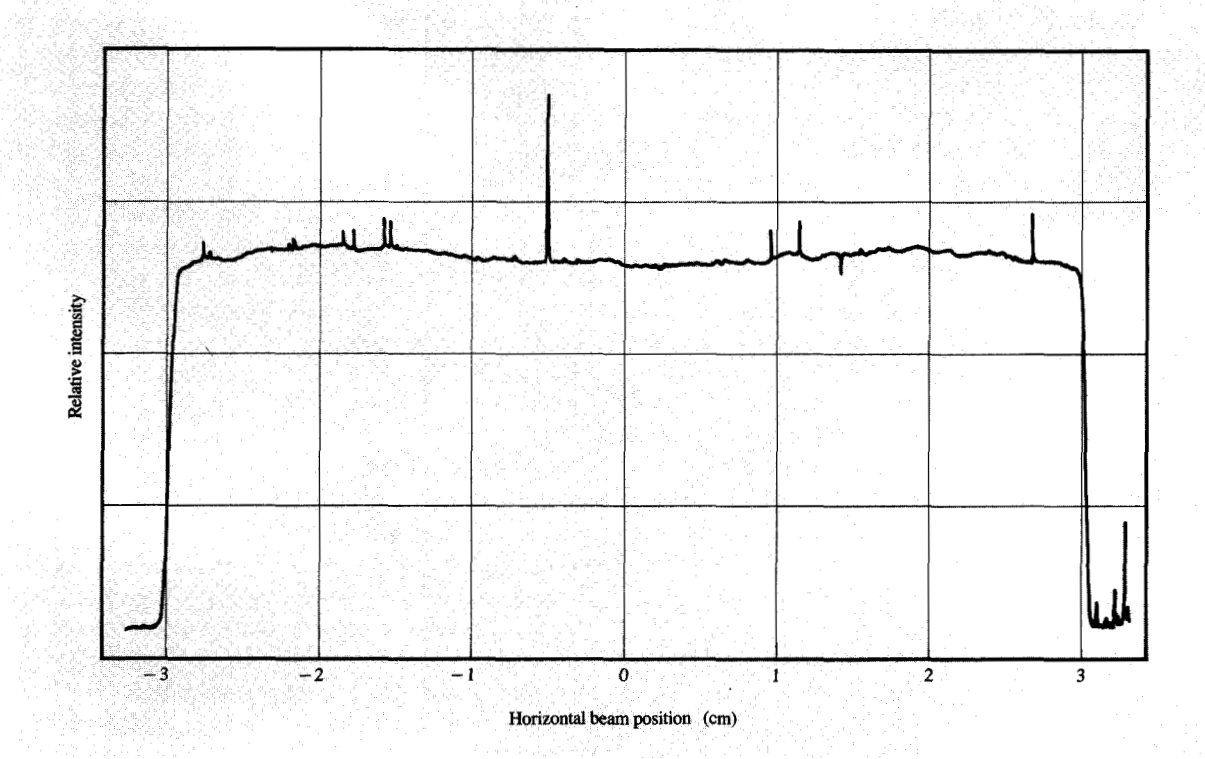


Figure 14

Measured horizontal uniformity of beam reflected from paraboloid mirror with vignetting through $50-\mu$ m-thick beryllium exit window. The sharp spikes are due to dust on the film during measurement in the scanning densitometer.

A preliminary version of the paraboloid mirror was temporarily obtained for early testing in the RD beamline. This mirror had significant figure errors (larger than 25 waves in some places), although most of the profile errors were in the low spatial frequency range (periodicity >10 mm). The mirror was installed in the RD beamline and aligned by optimizing its performance. The resulting measured performance was in excellent agreement with the modeling, as summarized in Table 4. Note that the $\sim 5 \times$ increase in flux due to collimation would give a typical wafer-incident flux of ~40 mW/cm² over a 25-mm-high field if used in the ALF beamline, even with the upstream filter still in place. The uniformity of illumination was also measured by exposing a sheet of film. The result without the vignetting plate is shown in Figure 13(a); it clearly shows the expected intensity rise at the edges of the field, as well as structure due to the beryllium window. When the vignetting plate was installed and aligned, the uniformity improved significantly to about ±1% over the central 50 mm of the field, as seen in Figure 13(b), exposed with the beryllium window removed. The small falloff of intensity at the edges of the field is believed to be due to

Table 4 Measured mirror performance (stationary).

Test parameter	Modeled	Measurement
Edge flux increase (no vignetting)	13%	11–14%
Uniformity (vignetted, with no exit window, 60-mm-wide field)	N/A	±1.6%
Uniformity (vignetted, 50- μ m Be exit window, 60-mm-wide field)	±3%	±2.6%
Flux gain (compared to planar mirror)	5.2×	5.3×
Beam width $(\pm 3\sigma)$	10 mm	10–11 mm
Beam profile sag	7 mm	7 mm

figure errors of the mirror, since these regions are where the figure errors were independently measured to be largest. Finally, the uniformity measured with a 50- μ m-thick beryllium window is shown in Figure 14.

407

It shows somewhat worse nonuniformity of about $\pm 2.6\%$ due to thickness variations in the window. Following these measurements, the mirror was returned to the vendor for further grinding and polishing. It should also be noted that because of spectral effects, the uniformity as measured in exposed photoresist may be different from that measured in film; resist measurements will be made after a mirror is permanently installed.

Future efforts

The primary goal for the near term is to install and characterize the final paraboloid mirrors for stationary use with the steppers. In addition, scanning mirrors will be investigated, with emphasis on characterization of the scanning performance of the paraboloid. Other optical systems, however, continue to be investigated. For example, the effective divergence of the X-ray beam at a point on the wafer and the effect of this divergence on resolution and process latitude have recently become topics of great interest. Controlling that divergence, however, is not an easy task, and a beamline that allowed the divergence to be varied would allow experiments to improve understanding of the effects. A beamline with optimized divergence might then be possible to design. Another desirable beamline capability would be the ability to vary the magnification of the printed image, for example by varying the runout in a controlled fashion. We are continuing to investigate designs which may provide these capabilities. The relatively high cost of paraboloid mirrors (compared to toroids, for example) has also led to further studies of potentially less expensive multimirror systems.

Exit windows are another area for future investigation. As noted above, the nonuniformity introduced by the beryllium window was significantly larger than that caused by the mirror itself. With a proper mirror scanning system, the window is now the largest source of nonuniformity, and in fact its contribution exceeds the total uniformity error budget that will be permitted in the future. Improved materials may provide a less grainy, more uniformly thick window. Alternatively, it should be possible to use a mechanical system (e.g., oscillating the window itself) to average out the small-scale nonuniformities. Convenient real-time flux detectors would also be valuable for measuring both dose and uniformity. The ideal flux detector would be stable and repeatable, accurately reflect flux changes at the wafer plane due to motion of the beam (if any), and measure the lithographically useful portion of the spectrum.

Conclusions

Beamlines of two different designs have been constructed and are now in operation in the ALF. They have met the vacuum requirements and are in routine use. With a planar mirror in the ALF beamline, the typical flux for a 25-mm-high field is 8 mW/cm 2 . The measured performance of the paraboloid mirror optics is in good agreement with the modeling and meets the design goals for the system. In particular, the >5× increase in flux due to the collimation will provide flux of >40 mW/cm 2 over the 25-mm-high field, consistent with providing exposure times of ~1 s when used with sensitive resists. Uniformity of ~3% has been achieved, with the beryllium exit window being the largest source of nonuniformity. Final installation of the paraboloid mirrors is awaiting their delivery and characterization. Future work will focus on scanning mirrors, alternative optical designs, and improved exit windows.

Acknowledgments

The authors wish to acknowledge the efforts of many of their colleagues in the design and installation of the beamlines. A. Palumbo and J. Granlund were responsible for the overall design and implementation of the control systems. R. Ruckel, M. Fisher, and M. Brandon provided many of the detailed designs for vacuum chambers and component assemblies. The ray-tracing program used for some of the optics modeling was written by D. Katcoff. M. Thompson of Motorola Corporation also participated in the design of the paraboloid optics. The beamline and front-end installation was handled largely by R. Ruckel, R. Scott, C. Schneider, J. Stuart, B. Hill, and C. Archie.

FIX DMACS is a trademark of Intellution, Inc. POMS is a registered trademark of Industrial Computing Designs Corporation.

PS/2 and OS/2 are registered trademarks of International Business Machines Corporation.

References

- 1. Julian Schwinger, "On the Classical Radiation of Accelerated Electrons," *Phys. Rev.* **75**, 1912–1925 (1949).
- 2. For a good summary of the properties of synchrotron radiation, see *Synchrotron Radiation Research*, Herman Winnick and S. Doniach, Eds., Plenum Press, New York, 1980, pp. 11-25.
- J. P. Silverman, V. DiMilia, D. Katcoff, K. Kwietniak, D. Seeger, L. K. Wang, J. M. Warlaumont, A. D. Wilson, D. Crockatt, R. Devenuto, B. Hill, L. C. Hsia, and R. Rippstein, "Fabrication of Fully Scaled 0.5-μm n-Type Metal-Oxide Semiconductor Test Devices Using Synchrotron X-Ray Lithography: Overlay, Resist Processes, and Device Fabrication," J. Vac. Sci. Technol. B 6, 2147-2152 (1988).
- E. Cullman and K. Cooper, "Experimental Results with a Scanning Stepper for Synchrotron-Based X-Ray Lithography," J. Vac. Sci. Technol. B 6, 2132-2134 (1988).
- R. P. Haelbich, J. P. Silverman, and J. Warlaumont, "Synchrotron Radiation X-Ray Lithography," Nucl. Instr. & Meth. 222, 291-301 (1984).
- Jerome P. Silverman, Rolf P. Haelbich, and John M. Warlaumont, "Synchrotron Radiation X-Ray Lithography: Recent Results," Proc. SPIE 448, 50-59 (1984).

- A. Flamholz and R. Rippstein, "X-Ray Stepper Exposure System Performance and Status," J. Vac. Sci. Technol. B 8, 2002–2007 (1990).
- R. P. Rippstein, D. L. Katcoff, and J. M. Oberschmidt, "Design of an X-Ray Lithography Beamline," *Proc. SPIE* 1089, 252–259 (1989).
- S. Hoffman, S. Nash, R. Ritter, and W. Smith, "Fabrication of a 1 Mbit Dynamic Random Access Memory with Four Levels Using X-Ray Lithography," J. Vac. Sci. Technol. B 9, 3241-3244 (1991).
- M. Bieber, H.-U. Scheunemann, H. Betz, and A. Heuberger, "Investigations of X-Ray Exposure Using Plane Scanning Mirrors," J. Vac. Sci. Technol. B 1, 1271-1275 (1983).
- K. Fujii, K. Okada, M. Nagano, and H. Kuroda, "Precisely Controlled Oscillating Mirror System for Highly Uniform Exposure in Synchrotron X-Ray Lithography," J. Vac. Sci. Technol. B 6, 2128-2131 (1988).
- H. Tanino, K. Hoh, M. Hirata, N. Atoda, and S. Ichimura, "Proposals and Experiments on Large Area Exposure in Synchrotron Radiation Lithography," J. Vac. Sci. Technol. B 3, 232-236 (1985).
- F. Cerrina, H. Guckel, J. D. Wiley, and J. W. Taylor, "A Synchrotron Radiation X-Ray Lithography Beam Line of Novel Design," J. Vac. Sci. Technol. B 3, 227-231 (1985).
- R. Cole and F. Cerrina, "Novel Toroidal Mirror Enhances X-Ray Lithography Beamline at CXrL," Proc. SPIE 1465, 111-121 (1991).
- R. Cole, P. Anderson, G. M. Wells, E. Brodsky, K. Yamazaki, and F. Cerrina, "Performance of the CXrL Beamlines," *Proc. SPIE* 1671, 461-470 (1992).
- T. Kitayama, T. Hayasaka, H. Yoshihara, and S. Ishihara, "Synchrotron X-Ray Lithography System Using a Compact Source," Proc. SPIE 1089, 159-163 (1989).
- Takashi Kaneko, Yasunao Saitoh, Seiichi Itabashi, and Hideo Yoshihara, "High Efficiency Beamline for Synchrotron Radiation Lithography," J. Vac. Sci. Technol. B 9, 3214-3217 (1991).
- L. G. Lesoine, K. W. Kukkonen, and J. A. Leavey, "ALF: A Facility for X-Ray Lithography," Proc. SPIE 1263, 131-139 (1990).
- D. E. Andrews, M. N. Wilson, A. I. Smith, V. C. Kempson, A. L. Purvis, R. J. Anderson, A. S. Bhutta, and A. R. Jorden, "Helios: A Compact Superconducting X-Ray Source for Production Lithography," *Proc. SPIE* 1263, 124-130 (1990).
- James M. Oberschmidt, Robert P. Rippstein, Raymond R. Ruckel, Alek C. Chen, John I. Granlund, and Alfred E. Palumbo, "Design of Synchrotron X-Ray Lithography Beamlines," Proc. SPIE 1671, 324-337 (1992).
- J. M. Shaw and M. Hatzakis, "Dosimetry for Lithographic Applications," J. Vac. Sci. Technol. 19, 1343-1347 (1981).
 C. N. Archie, J. I. Granlund, R. W. Hill, K. W.
- C. N. Archie, J. I. Granlund, R. W. Hill, K. W. Kukkonen, J. A. Leavey, L. G. Lesoine, J. M. Oberschmidt, A. E. Palumbo, C. Wasik, M. Q. Barton, J. P. Silverman, J. M. Warlaumont, A. D. Wilson, R. J. Anderson, N. C. Crosland, A. R. Jorden, V. C. Kempson, J. Schouten, A. I. C. Smith, M. C. Townsend, J. Uythoven, M. C. Wilson, M. N. Wilson, D. E. Andrews, R. Palmer, R. Webber, and A. J. Weger, "Installation and Early Operating Experience with the Helios Compact Synchrotron X-Ray Source," J. Vac. Sci. Technol. B 10, 3224 (1992).
- Chas Archie, "Performance of the IBM Synchrotron X-Ray Source for Lithography," IBM J. Res. Develop. 37, 373-384 (1993, this issue).
- B. Lai and F. Cerrina, "SHADOW: A Synchrotron Radiation Ray Tracing Program," Nucl. Instrum. & Meth. A 246, 337-341 (1986).

Received November 20, 1992; accepted for publication April 22, 1993

Jerome P. Silverman IBM Semiconductor Research and Development Center, Thomas J. Watson Research Center, P.O. Box 218, Yorktown Heights, New York 10598 (AGMAN at YKTVMV, agman@watson.ibm.com). Dr. Silverman is a Research Staff Member and Manager in the Advanced Lithography Systems Department of the Semiconductor Research and Development Center. He received a B.S. degree (1973) and a Ph.D. degree (1978), both in physics, from the Massachusetts Institute of Technology. He joined the IBM Research Division in 1981 as a Research Staff Member. For his early work he was in residence at Brookhaven National Laboratory, where he helped build, commission, characterize and operate IBM's first X-ray lithography beamline. He was subsequently responsible for the characterization, modification, and operation of the IBM stepper installed at the beamline, which was used for the first circuits fabricated using synchrotron radiation X-ray lithography for all exposure levels. He currently manages the group responsible for the beamlines in the IBM Advanced Lithography Facility, as well as for the performance of the storage ring. Dr. Silverman has received an IBM Outstanding Technical Achievement Award and an IBM Research Division Technical Group Award for his work in X-ray lithography.

Robert P. Rippstein IBM Semiconductor Research and Development Center, Rte. 52, Hopewell Junction, New York 12533 (RIPPSTEI at FSHVMX). Mr. Rippstein is an Advisory Engineer currently involved with X-ray optics and beamline development at the Advanced Lithography Facility on the IBM East Fishkill site. He received his B.S. degree in physics in 1970 and his M.S. degree in photographic science in 1971, both from the Rochester Institute of Technology. After joining IBM in 1977, he worked on copier optics and illumination and step-and-repeat optical lithography. He has worked on X-ray lithography tooling development since 1987.

James M. Oberschmidt IBM Semiconductor Research and Development Center, Rte. 52, Hopewell Junction, New York 12533 (OBERSCHM at FSHVMX, oberschm@fshvmx.vnet.ibm.com). Dr. Oberschmidt is an Advisory Engineer who has been working in X-ray lithography tool and process development since 1987. He received his B.S.

degree in physics from the University of Cincinnati in 1974 and his M.S. and Ph.D. degrees in physics from the University of Illinois at Champaign-Urbana in 1976 and 1980, respectively. From 1979 to 1981 he worked at the IBM Thomas J. Watson Research Center on materials science and engineering for integrated circuit interconnection. From 1981 to 1985 he worked in the IBM Advanced Packaging Technology Laboratory in East Fishkill, New York, on interconnection technology and high-performance packaging technology. In 1985 and 1986 he worked on the technical staff of the East Fishkill semiconductor manufacturing plant manager and in semiconductor process strategies. Dr. Oberschmidt has published papers related to each of the areas in which he has worked and has several patents in packaging technology, having achieved IBM's first invention plateau. He is a member of the American Physical Society.